MASTER

MATHEMATICAL FINANCE

MASTER'S FINAL WORK

DISSERTATION

Jump-Diffusion Modeling In Emission Markets Through An Integro-Differential Equation

Miguel Alexandre Gomes Falcão

SUPERVISION:

João Guerra

JUNE 2025

Table of Contents

List of Figures

Acknowledgements

I would like to express my deepest gratitude to my advisor, João Guerra, for his guidance, support, and availability throughout the development of this thesis.

I am also immensely thankful to my friends who have accompanied me on this academic journey and supported me through challenging times. A special thanks goes to Leonor, who has always been there for me.

Finally, I wish to extend my heartfelt appreciation to my family, particularly my parents and sisters, for their unconditional support throughout my life.

Glossary

PIDE - Partial Integro-Differential Equation

EU - European Union

EU ETS - European Union Emission Trading System

CO_2 - Carbon Dioxide

Abstract

In this thesis, will be explored how emission allowance prices evolve in carbon markets, using mathematical models that account for both gradual changes and sudden shocks. Inspired by the work of [5], the study replicates the results based on a jump-diffusion model with standard normally distributed jumps. Then it goes further by testing two alternative models, the Double Exponential and CGMY distributions, that aim to better reflect the real behavior of the market, particularly in situations of extreme volatility. The model is solved numerically using the finite difference method, with all simulations implemented in Python. By comparing the effects of different jump distributions, the thesis provides insights into how these models can help price emission-related financial derivatives more accurately and support better decision-making in systems like the EU Emissions Trading Scheme (EU ETS).

1 Introduction

1.1 Context and Relevance

The growing concern about the increase in global warming has intensified in recent years, which led to the urgency for the development and creation of new economic mechanisms for the reduction of greenhouse gas emissions, such as CO_2. One of the main mechanisms developed was the Emissions Trading Scheme (ETS), considered as one of the most effective tools for the mitigation of carbon dioxide. In this context, one of the most important and the largest carbon market in the world is the European Union Emissions Trading Scheme (EU ETS), which is based on the cap-and-trade principle, that ensures the reduction of emissions by companies. The main objective of this type of market is to comply with environmental proposals, such as, for example, the Kyoto Protocol. For this purpose, the EU ETS establishes a price for carbon emissions, which encourages their reduction by market participants.

The fundamental principle behind this type of market is simple: a regulatory authority establishes a maximum limit (cap) for the total that can be emitted during a compliance period. For this, it distributes or auctions emission certificates, each one allowing its holder to emit one ton of CO_2. Thus, at the end of the compliance period, if companies do not have enough certificates to cover the total emitted, they will be subject to a penalty. For that, companies can trade certificates among themselves, adopting the best strategy that optimizes their portfolios. To know more about these markets, see [1], [2], [3] and [4].

Therefore, it becomes essential to determine the evolution of the prices of emission certificates, as these are quite volatile, influenced by several factors, such as changes in the allocation of these certificates, political changes, creation of new more sustainable technologies, changes in the energy market, etc.

In this way, the use of complex mathematical models becomes essential, as they can reflect the uncertainty associated with these markets. Thus, in this thesis, the mathematical model proposed in the article “Jump-Diffusion Modeling in Emission Markets” by Borovkov, Decrouez and Hinz [5] will be adopted, where a mathematical model based on jump-diffusion processes is presented to represent the evolution of these prices. Furthermore, by considering abrupt movements in the market, the article will implement jumps in the model, which will result in integro-differential equations. This methodology offers a useful tool to analyze the volatility associated with this type of market, which will reflect in a more realistic and more accurate price for these emission certificates.

1.2 Main goal of the Thesis

The main goal of this thesis is to develop a mathematical model to simulate the price of emission allowances, based on the foundational work of Borovkov et al. [5]. Initially, the discrete-time framework will be presented, as a foundational step for the continuous and jump-diffusion models developed in this thesis. Thus, this study aims to reproduce the evolution of certificate prices for different times to maturity and under different parameters, using a standard normal distribution for the jumps, and later extending the original work by integrating other distributions such as the Double Exponential and a CGMY Model in the modeling of jumps, which will allow drawing conclusions suitable to different market conditions. After the discretization of the partial integro-differential equation (PIDE) associated to the pricing problem, it will be possible to analyze the impact of the different distributions used on emission allowance prices and their implications for derivative valuation.

1.3 Structure of the Thesis

This thesis has six main chapters, followed by references and appendices:

- Chapter 1 - Introduction.
- Chapter 2 – Theoretical Background: The second chapter examines the fundamental principles of emission markets, with particular emphasis on the structure and functioning of the European Union Emissions Trading System (EU ETS). It introduces the concept of jump-diffusion processes and discusses the properties of the jump distributions considered: the Standard Normal, Double Exponential, and CGMY Model.
- Chapter 3 – Methodology: In this chapter, the mathematical model proposed by Borovkov et al. [5] is outlined, along with a detailed explanation of the numerical discretization of the partial integro-differential equation (PIDE) using the finite difference method.
- Chapter 4 – Results and Discussion: In this Section, the results are presented for each jump distribution. A comparison with the findings of the original article is provided, as well as an analysis of numerical and theoretical differences. The implications of the different jump distributions are interpreted, model limitations are discussed, and practical applications within emission markets are explored.
- Chapter 5 – Conclusions: The main contributions of the thesis are summarized, advances in emission allowance price modeling are highlighted, and possible directions for future research are proposed.
- References and Appendices: A complete bibliography is provided, along with detailed simulation parameters, and additional figures that support the analysis.

2 Theoretical Background

Carbon emission markets have emerged as a response to growing environmental concerns, particularly regarding global warming driven by greenhouse gas emissions such as carbon dioxide (CO_2). However, these markets are characterized by highly volatile prices, necessitating the use of advanced mathematical models to accurately capture their dynamics.

In this chapter, the theoretical foundation for modeling emission allowance price dynamics using jump-diffusion processes will be established. This section will first provide an overview of how emission markets operate, followed by a discussion of the core principles underlying jump-diffusion processes. Finally, the distinctive features of various jump distributions: the Standard Normal, Double Exponential, and CGMY model will be examined in detail and some definitions will be presented.

2.1 Carbon Emission Markets

Created in 2005, the European Union Emissions Trading System (EU ETS) is the first carbon market in the world, being one of the largest at a global level. As mentioned earlier in this thesis, the EU ETS is based on the cap and trade principle. The cap refers to the maximum limit allowed to be emitted by the market participants during the compliance period, where this limit is reduced every year in order to reach the proposed environmental goals. Additionally, this total emission limit is expressed in emission allowances, as each one gives the company that owns it the right to emit one tonne of CO_2. These allowances are either distributed for free or auctioned at the beginning of the compliance period and they can be traded between companies. Since the cap decreases, the supply of allowances to the EU carbon market also decreases.

All market agents are required to monitor and report their annual emissions, and they must hold enough certificates to cover all of their emissions. If they do not hold enough certificates, they will be subject to a heavy penalty. On the other hand, if they manage to reduce their emissions, firms can sell the remaining allowances or keep them for the future.

So, it's expected that the price of these certificates is quite volatile, being influenced by both external market factors, like geopolitical events, and internal events, such as changes in the allocation of these certificates.

This level of unpredictability highlights the importance of using complex and sophisticated models to accurately price emission allowances and related financial instruments, such as European options. These tools are essential for effective risk management and play a key role in the strategies of market participants and policymakers within the carbon trading space.

2.2 Jump Diffusion Processes

Jump-diffusion processes are advanced stochastic models designed to capture the complex behavior of price evolution in financial markets. This processes integrates a diffusion component, modeled by Brownian motion, with discrete jumps governed by a Poisson process. The Brownian motion captures gradual price fluctuations, while the Poisson process introduces sporadic jumps, reflecting sudden shocks caused by external events. By integrating both smooth and abrupt movements, jump-diffusion frameworks provide a more comprehensive and realistic description of assets that are prone to volatility. This dual approach is particularly effective for modeling markets where unexpected shocks can cause significant and immediate impacts, offering valuable insights for risk assessment and strategic decision making.

2.2.1 Apllication in Emission Markets

As previously noted, carbon markets are highly susceptible to unpredictable events, leading to sudden price shifts in emission allowances that traditional continuous diffusion models fail to adequately capture. Jump diffusion models effectively integrate both the market's inherent volatility and discrete, abrupt price movements, providing a more accurate representation of price dynamics. This is critical for the fair pricing of financial derivatives, such as options and futures, and for gaining deeper insights into market behavior under risk scenarios. In addition, these models enable the development of more effective risk and hedging strategies. By employing jump-diffusion processes, stakeholders can better navigate the uncertainty and complexity of emission markets, fostering more efficient and sustainable management of both financial and environmental risks.

2.3 Definitions

In this section will be introduced some key definitions, presented in [6] and [7], essential for understanding the concepts discussed in this thesis and some of them will also be applied throughout the analysis.

We will consider a filtered probability space $(\Omega, \mathcal{F}, \mathbb{P}, \{\mathcal{F}_t\}_{t\geq 0})$.

2.3.1 Lévy Process and Lévy Measure

An adapted stochastic process $L = \{L_t, t \in [0, T]\}$ is a Lévy process if:

- $L_0 = 0$ a.s.
- L has independent increments
- L has stationary increments
- L is stochastically continuous, i.e., for every $t \in [0, T]$ and $\varepsilon > 0$, we have

$$\lim_{s\to t} \mathbb{P}(|L_t - L_s| > \varepsilon) = 0.$$

Let ν be a Borel measure defined on $\mathbb{R} \setminus \{0\}$. We say that ν is a Lévy measure if

$$\int_{\mathbb{R}\setminus\{0\}} (|x|^2 \wedge 1)\, \nu(dx) < \infty \tag{1}$$

2.3.2 Infinite divisible distributions

A probability distribution μ on $\mathbb{R}$ is said to be infinitely divisible if for any $n \in \mathbb{N}$, there exist n independent and identically distributed (i.i.d.) random variables $Y_1^{(n)}, Y_2^{(n)}, \ldots, Y_n^{(n)}$ such that:

$$Y_1^{(n)} + Y_2^{(n)} + \cdots + Y_n^{(n)} \sim \mu. \tag{2}$$

The following formula, called the Lévy-Khintchine formula, provides a fundamental characterization of infinitely divisible distributions.

P_X is infinitely divisible if and only if there exists a triplet (b, c, ν), $b \in \mathbb{R}, c \geq 0$, where ν is a Lévy measure, $\nu(\{0\}) = 0$ and

$$\mathbb{E}\left[e^{iuX}\right] = \exp\left[ibu - \frac{u^2 c}{2} + \int_{\mathbb{R}} \left(e^{iux} - 1 - iux\mathbf{1}_{\{|x|<1\}}\right)\, \nu(dx)\right]. \tag{3}$$

2.3.3 Itô Process

An Itô process is a stochastic process of the form $X_t = X_a + \int_a^t f(s)dB(s) + \int_a^t g(s)ds$, where B is a Standard Brownian Motion, $a \leq t \leq b$, X_a is $\mathcal{F}_a$-measurable, $f \in H^2_{ad}\left\{[a,b] \times \Omega\right\}$ and $g \in H^1_{ad}\left\{[a,b] \times \Omega\right\}$ are adapted and measurable processes. These spaces of processes are defined as:

$$H^2_{ad}\left\{[a,b] \times \Omega\right\} := \left\{f : [a,b] \times \Omega \to \mathbb{R} \text{ measurable and adapted: } P\left[\int_a^b |f(s)|^2 ds < \infty\right] = 1\right\},$$
$$H^1_{ad}\left\{[a,b] \times \Omega\right\} := \left\{g : [a,b] \times \Omega \to \mathbb{R} \text{ measurable and adapted: } P\left[\int_a^b |g(s)| ds < \infty\right] = 1\right\}.$$

2.4 Distributions

2.4.1 Normal Distribution

The Normal distribution is widely employed in financial modeling due to its simplicity and analytical properties. It is defined by the following probability density function:

$$f(x) = \frac{1}{\sqrt{2\pi\sigma^2}} \exp\left(-\frac{(x-\mu)^2}{2\sigma^2}\right). \tag{4}$$

Key Statistical Properties ($X \sim N(\mu, \sigma^2)$):

- Expected Value: $E[X] = \mu$ - Represents the average shift of jumps.
- Variance: $Var[X] = \sigma^2$ - Measures the dispersion of jump sizes around the mean.

The Normal distribution is symmetric around its mean, with tails that decay exponentially, implying that extreme jumps, whether positive or negative, are less likely. Consequently, this distribution is suitable for modeling moderate shocks, as its light tails fail to adequately capture the probability of extreme jumps, which are common in volatile markets.

2.4.2 Double Exponential Distribution

The Double Exponential Distribution is defined by the following probability density function, as presented by [8]:

$$f(y) = p\eta_1 e^{-\eta_1 y} \mathbb{1}_{\{y \geq 0\}} + q\eta_2 e^{\eta_2 y} \mathbb{1}_{\{y<0\}}, \tag{5}$$

where $p, q > 0$, $p + q = 1$, represent the probabilities of upward and downward jumps, and $\eta_1 > 1$, $\eta_2 > 0$ control the exponential decay rates for positive and negative jumps, respectively. In other words,

$$\log(V) = Y \stackrel{d}{=} \begin{cases} \xi^+, & \text{with probability } p \\ -\xi^-, & \text{with probability } q \end{cases}$$

where ξ^+ and ξ^- are exponential random variables with means $1/\eta_1$ and $1/\eta_2$, respectively.

Key Statistical Properties ($Y \sim$ Double Exponential):

- $E(Y) = \frac{p}{\eta_1} - \frac{q}{\eta_2}$ - Reflects the asymmetry between positive and negative jumps.
- Variance: $Var[Y] = pq\left(\frac{1}{\eta_1} + \frac{1}{\eta_2}\right)^2 + \frac{p}{\eta_1^2} + \frac{q}{\eta_2^2}$ - Depends on the decay rates and the probabilities p e q.

This distribution effectively captures asymmetries, such as pronounced upward jumps driven by stricter regulations in the EU Emissions Trading System (EU ETS) or energy crises, for instance. Since the double exponential distribution features heavier tails compared to the Normal distribution, it provides a more realistic modeling framework by assigning higher probabilities to extreme events, such as revisions in allowance allocations.

2.4.3 CGMY Distribution

The CGMY(C, G, M, Y) distribution, as presented in [9] and discussed in [7], is a four-parameter distribution where the Lévy measure is given by:

$$\nu_{\text{CGMY}}(dx) = \begin{cases} C\exp(Gx)(-x)^{-1-Y}\,dx, & x < 0, \\ C\exp(-Mx)x^{-1-Y}\,dx, & x > 0. \end{cases} \tag{6}$$

The CGMY distribution is infinitely divisible and we can define the CGMY Lévy process $X^{(\text{CGMY})} = \{X_t^{(\text{CGMY})}, t \geq 0\}$ as the process that starts at zero, has independent and stationary increments, and is characterized by the property that the increment over a time interval of length s follows a CGMY(sC, G, M, Y) distribution. In other words, the characteristic function of $X_t^{(\text{CGMY})}$ is given by:

$$\mathbb{E}\left[e^{iuX_t^{(\text{CGMY})}}\right] = \phi_{\text{CGMY}}(u; tC, G, M, Y) = \left(\phi_{\text{CGMY}}(u; C, G, M, Y)\right)^t,$$

where

$$\phi_{\text{CGMY}}(u; C, G, M, Y) = \exp\left(C\Gamma(-Y)\left((M - iu)^Y - M^Y + (G + iu)^Y - G^Y\right)\right),$$

which can be expressed as:

$$\mathbb{E}\left[e^{iuX_t^{(\text{CGMY})}}\right] = \exp\left(Ct\Gamma(-Y)\left((M - iu)^Y - M^Y + (G + iu)^Y - G^Y\right)\right). \tag{7}$$

Each parameter in the CGMY process has a specific role.

The parameter C controls the overall activity level of the process. It can be calibrated to adjust the aggregate activity and influences the kurtosis of the distribution.

The parameters G and M control the exponential decay rates in the Lévy density, with G affecting the right tail and M controlling the left. The difference between G and M introduces skewness in the distribution, with G > M resulting in a heavier left tail. In the special case when G = M , the Lévy measure is symmetric. Their sum measures the magnitude of large versus small moves, while their difference affects the relative frequency of upward versus downward movements.

The parameter Y is crucial to determine the fine structure of the process. It influences the monotonicity of the jumps and the overall level of activity, which may be finite or infinite. Y is the key to understanding the behavior of both jumps up and down and the overall variation of the process.

Following, we have some interesting properties of the CGMY process:

1. The CGMY Process is a pure jump process, that is, it contains no Brownian part ($\sigma = 0$).
2. Mean: $C(M^{Y-1} - G^{Y-1})\Gamma(1 - Y)$
3. Variance: $C(M^{Y-2} + G^{Y-2})\Gamma(2 - Y)$

The CGMY model excels in capturing both high-frequency small jumps (infinite activity) and heavy-tailed distributions, making it ideal for modeling extreme events like regulatory shocks or energy crises that trigger significant price swings in the EU Emission Trading System (EU ETS). Its robust ability to represent tail risks is especially relevant for emission markets, where sudden policy shifts or market disruptions can lead to pronounced volatility, enhancing the accuracy of risk assessment and pricing of emission-related derivatives.

3 Methodology

3.1 Modeling Emission Markets in Discrete Time

This section presents the discrete-time framework for modeling emission markets, based on Borovkov et al [5], as a foundational step for the continuous and jump-diffusion models developed in this thesis.

During the compliance period, each participant in the Emission Trading Scheme (ETS) dynamically adjusts their production processes (and, consequently, their emissions) to maximize their revenue, and, since we assume that we are at a discrete time, the trades of emission certificates occur at discrete points in times $t = 0, 1, 2, \ldots, T < \infty$. In this context, the price of allowances reaches an equilibrium determined by the supply and demand of emission allowances. The following analysis is based on the model from [5], which characterizes equilibrium allowance prices in terms of non-compliance uncertainty and emission reduction costs, serving as the starting point for this investigation.

Consider a filtered probability space $(\Omega, \mathcal{F}, \mathbb{P}, \{\mathcal{F}_t\}_{t=0}^T)$, in which all analyzed processes are adapted to the filtration $\{\mathcal{F}_t\}_{t=0}^T$. This probabilistic framework serves as the foundation for modeling the dynamics of a market composed of a finite set I of agents subject to the rules of the Emission Trading Scheme (ETS), whose interactions determine the equilibrium prices of emission allowances.

From now on, several definitions that will be useful for modeling the price of emission allowances will be presented.

Emissions

Each agent $i \in I$ is characterized by a stochastic process $\{E_t^i\}_{t=0}^{T-1}$, where each $\{E_t^i\} = \{E_t^i\}(\omega)$ represents the total emissions of agent i during the time interval $(t, t+1]$ if the agent does not apply abatement measures.

Reduction

The process ξ_t^i represents the total units that the agent i will reduce during $(t, t+1]$, strategically adjusting to comply with regulatory requirements.

Cost of Reduction

Each unit of emission reduction is associated with a cost, modeled by a function $C_t^i(x)$, which is strictly convex and continuous with $C_t^i(0) = 0$. Thus, for a reduction of x units of pollutant during the interval $(t, t+1]$, the associated cost is $C_t^i(x)$. This function reflects uncertainties in factors such as fuel prices, resulting in a total abatement cost up to the compliance deadline T, given by:

$$\sum_{t=0}^{T-1} C_t^i(\xi_t^i). \tag{8}$$

Reduction Volume

For each agent i, the following function is defined:

$$r_t^i(a) = \arg\max\{ax - C_t^i(x) : x \in [0, E_t^i]\}. \tag{9}$$

This function identifies the "locally optimal" reduction volume for agent i during the interval $(t, t+1]$, based on the price of one allowance unit set at $a > 0$ for that period, which is equivalent to say that if we assume that all the agents are rational, then we have that this value will be the level of emission reduction that they will adopt.

Transaction Costs

Considering the process θ_t^i as the change in the number of licenses held by the agent i at time t and supposing that emission licenses are traded at the spot price A_t, for each time t, we have that the total trading cost for agent i is given by:

$$\sum_{t=0}^{T} \theta_t^i A_t. \tag{10}$$

From now on, for simplicity, it is assumed that the interest rate is zero, which is equivalent to considering already discounted prices.

Total Pollution

With the information we have above, the total pollution of the agent i will be given by the difference between the total emitted and the total that the agent reduced in the compliance period:

$$\sum_{t=0}^{T-1} E_t^i - \sum_{t=0}^{T-1} \xi_t^i. \tag{11}$$

Total Loss

Let γ_i be the initial allowance allocation for agent i. Then the loss incurred by agent i due to a potential penalty payment (π - the penalty for emissions equivalent to one allowance), is given by:

$$\pi \left[\sum_{t=0}^{T-1}(E_t^i - \xi_t^i - \theta_t^i) - \gamma^i - \theta_T^i\right]^+ . \tag{12}$$

Feasible Strategy Space

Finally, we define the space of feasible trading strategies and abatement strategies.

Definition of Strategies:

- Trading Strategy ($\theta^i = \{\theta_t^i\}_{t=0}^{T}$): Each agent $i \in I$ can dynamically adjust the number of emission certificates they hold throughout the compliance period.
- Emission Reduction Strategy ($\xi^i = \{\xi_t^i\}_{t=0}^{T-1}$): Each agent $i \in I$ can decide to reduce their emissions during the compliance period.

Thus, the feasible strategy space for agent i can be defined as:

$$\mathcal{U}^i := \{(\theta^i, \xi^i) : 0 \leq \xi_t^t \leq E_t^i, t = 0, \ldots, T-1\}.$$

These restrictions ensure that the strategies are realistic and viable, as the volume of reduced emissions cannot exceed the initial emissions of the agent.

To specify risk preferences, we will describe the investor's attitude toward risk through individual utility functions U^i, where $i \in I$. Thus, the expected utility of the agent i is given by:

$$u^i(X) = \mathbb{E}[U^i(X)],$$

where $U^i(X)$ is continuous, strictly increasing and concave. Thus, agent i acts rationally by choosing the strategy (θ^i, ξ^i) that maximizes their expected utility:

$$u^i(L^{A,i}(\theta^i, \xi^i)),$$

where

$$L^{A,i}(\theta^i, \xi^i) := -\sum_{t=0}^{T-1}(\theta_t^i A_t + C^i(\xi_t^i)) - \theta_T^i A_T - \pi \left[\sum_{t=0}^{T-1}(E_t^i - \xi_t^i - \theta_t^i) - \gamma^i - \theta_T^i\right]^+ \tag{13}$$

denotes the total revenue of agent i.

To continue this theoretical framework is essential to present the concept of market equilibrium.

Definition 1: Market Equilibrium

A market is described by the so-called equilibrium if:

- The price of certificates is determined by the strategic interaction of all agents.
- Each agent is satisfied with their strategy.

- Each agent optimize their own utility function under the prevailing market conditions $u^i(L^{A,i}(\theta^i, \xi^i))$.

This equilibrium concept is essential to ensure that the model reflects real market conditions, where prices appropriately reflect supply and demand, and no agent has an incentive to change their strategy given the decisions of the other agents.

Now we are ready to define what an equilibrium certificate price process is ($A^* = \{A_t^*\}_{t=0}^T$), which is crucial to understanding how the model captures the equilibrium condition.

Definition 2:
An adapted process ($A^* = \{A_t^*\}_{t=0}^T$) is called an equilibrium certificate price process if, for each agent $i \in I$, there exists a strategy $(\theta^{*i}, \xi^{*i}) \in \mathcal{U}^i$ such that $u^i(L^{A^*,i}(\theta^{*i}, \xi^{*i})) < \infty$ and:

- The cumulative changes in positions are in zero net supply:

$$\sum_{i \in I} \theta_t^{*i} = 0 \text{ for all } t = 0, \ldots, T. \tag{14}$$

  This condition ensures that the market is balanced, meaning there is neither an excess nor a shortage of certificates. This reflects the fact that, in an efficient market, the total quantity of certificates bought must equal to the total quantity sold.

- Satisfaction with Own Strategy: Each agent $i \in I$ is satisfied with their own strategy in the sense that, for any other strategy $(\theta^i, \xi^i) \in \mathcal{U}^i$, the following holds:

$$u^i(L^{A^*,i}(\theta^{*i}, \xi^{*i})) \geq u^i(L^{A^*,i}(\theta^i, \xi^i)). \tag{15}$$

  This second condition ensures that each agent maximizes their expected utility by choosing the optimal combination of certificate trading and emission reduction.

In [10], this equilibrium concept was applied to simplify and construct a reduced-form model that outlines the development of allowance prices from a risk-neutral ($Q \sim P$) perspective. This method relies on the following three properties of the equilibrium described above:

- **Property (a): Absence of Arbitrage:** There are no arbitrage opportunities in the market, as any profitable strategy would be immediately adopted by all agents. This ensures that prices accurately reflect supply and demand conditions, with no gaps or inconsistencies that would allow unlimited risk-free gains.

- **Property (b): Optimality of Emission Reduction:** If a technology exists with emission reduction costs lower than the current certificate price, it becomes optimal to reduce emissions and sell certificates for profit. This reinforces the notion that agents act rationally, maximizing their financial benefits in response to market conditions.

- **Property (c):** At the end of the compliance period (T), only two final outcomes are possible for the certificate price: it drops to zero if there is an excess of certificates, or it rises to the penalty level if there is a shortage of certificates.

With some reasonable supplementary assumptions, [10] suggests that the conclusions above can be inferred from the equilibrium in the following way. This proposition is proved in [10].

Proposition 1:
Suppose that $\{A_t^*\}_{t=0}^T$ is an equilibrium allowance price process and $\{\xi_t^{*i}\}_{t=0}^{T-1}$, for $i \in I$, are the corresponding equilibrium abatement strategies. Then:

- a) There exists a measure $\mathbb{Q}$ equivalent to the original measure P such that $\{A_t^*\}_{t=0}^T$ is a martingale under $\mathbb{Q}$.
- b) For each $i \in I$, the following holds:

$$\xi_t^{*i} = r_t^i(A_t^*), \quad t = 0, \dots, T-1. \tag{16}$$

- c) The terminal value of the allowance price is given by:

$$A_T^* = \pi \mathbb{1}\left(\sum_{i \in I}\left(\sum_{t=0}^{T-1}(E_t^i - \xi_t^{*i}) - \gamma^i\right) \geq 0\right). \tag{17}$$

  The equality (17) ensures that, at the end of the compliance period, the certificate price depends on the difference between the total emissions $\sum_{t=0}^{T-1} E_t^i$ and the total reductions $\sum_{t=0}^{T-1} \xi_t^{*i}$, in addition to the initial allocations γ^i. Consequently, if there is a shortage of certificates, the price rises to the penalty level π; otherwise, it falls to zero.

To simplify, let us introduce the overall "business-as-usual" allowance shortage by:

$$\varepsilon_T = \sum_{i \in I}\left(\sum_{t=0}^{T-1} E_t^i - \gamma^i\right). \tag{18}$$

Since the terminal value A_T^* depends directly on the random variable ε_T, this variable also relies on the intermediate values $\{A_t^*\}_{t=0}^{T-1}$ of the certificate prices, as outlined in item b) of Proposition 1. Thus, by the martingale property of $\{A_t^*\}_{t=0}^T$, we have:

$$A_t^* = \pi \mathbb{E}^{\mathbb{Q}}\left[\mathbb{1}\left(\varepsilon_T - \sum_{t=0}^{T-1} r_t(A_t^*) \geq 0\right) \mid \mathcal{F}_t\right], \quad t = 0, \dots, T-1. \tag{19}$$

where

$$r_t(A_t^*) = \sum_{i \in I} r_t^i(a)$$

denotes the cumulative reduction function and a is the price of one allowance unit.

With this, the problem simplifies in specifying a random variable ε_T representing the cumulative allowance shortage and determining a $\mathbb{Q}$-martingale $\{A_t^*\}_{t=0}^{T-1}$ such that the terminal price satisfies:

$$A_T^* = \pi \mathbb{1}\left(\varepsilon_T - \sum_{t=0}^{T-1} r_t(A_t^*) \geq 0\right), \tag{20}$$

where $\mathbb{1}(\cdot)$ is the indicator function. This formulation ensures that the price reflects the balance between allowance supply and demand at the compliance horizon.

This discrete-time framework provides a foundation for understanding emission allowance price dynamics. Extending this approach to a continuous-time setting is a natural progression, as outlined in the following formulation. This transition simplifies the modeling process and sets the stage for incorporating jump-diffusion processes, which are essential for capturing market shocks.

That transition is straightforward and leads to a refined problem statement.

Given a probability measure $\mathbb{Q} \sim \mathbb{P}$ and a family of reduction functions $\{r_t\}_{t\in[0,T]}$, the objective is to:

- Specify a random variable ϵ_T that quantifies the total "business-as-usual" allowance shortage over the interval $[0, T]$.
- Determine a $\mathbb{Q}$-martingale $\{A_t^*\}_{t\in[0,T]}$ such that the terminal condition holds:

$$A_T^* = \pi \mathbf{1} \left(\varepsilon_T - \int_0^T r_s(A_s^*) ds \geq 0 \right). \tag{21}$$

This continuous-time approach enables the integration of stochastic processes, such as jump-diffusion, to model abrupt market changes. The problem simplifies to defining ε_T and $\{r_t\}_{t\in[0,T]}$, which can be calibrated using market data, thereby connecting the discrete and continuous frameworks examined in this thesis.

3.2 Modeling Emission Markets in Continuous Time

In this section, the continuous diffusion model is introduced to capture the evolution of emission allowance prices within a carbon market. The goal is to model these prices realistically, incorporating both continuous movements (diffusion) and discrete jumps (jump-diffusion), following the modelling approach in [5].

Consequently, this framework describes a scenario where the market may experience sudden changes due to the presence of jumps. A practical example is the EU ETS, where revised decisions on certificate allocations can lead to abrupt price jumps. Additionally, sudden shifts in demand or fuel prices can significantly affect pollution levels, directly impacting certificate prices.

The model assumes the following:

- The compliance period is a continuous interval $[0, T]$.
- All relevant stochastic processes are adapted to a filtered probability space $(\Omega, \mathcal{F}, \mathbb{Q}, \{\mathcal{F}_t\}_{t\in[0,T]})$ equipped with a risk-neutral probability measure $\mathbb{Q} \sim \mathbb{P}$.

This measure ensures that emission certificate prices are martingales under $\mathbb{Q}$, accurately reflecting market uncertainty without systematic expectations of gain or loss.

As previously discussed, the objective is to find a solution $\{A_t\}_{t\in[0,T]}$ such that:

$$A_t = \pi \mathbb{E}^{\mathbb{Q}} \left[\mathbb{1} \left(\epsilon_T - \int_0^t r_s(A_s)\, ds \geq 0 \right) \mid \mathcal{F}_t \right], \quad t \in [0, T]. \tag{22}$$

From the discrete time framework provided by [10], and assuming certain conditions:

- **Independence of Martingale Increments:** The increments of the martingale $\{\epsilon_t := \mathbb{E}^{\mathbb{Q}}(\epsilon_T \mid \mathcal{F}_t)\}_{t\in[0,T]}$ are independent;

- **Determinism and Time Independence of Reduction Functions:** The reduction functions $r_t : \mathbb{R}_+ \times \Omega \to \mathbb{R}_+$ are deterministic and independent of time.

it is reasonable to assume that the solution can be expressed in the functional form:

$$A_t = \alpha(t, X_t), \quad t \in [0, T], \tag{23}$$

where $\alpha : [0, T] \times \mathbb{R} \to \mathbb{R}$ is a suitable deterministic function. This simplification allows the certificate price to be described as a deterministic function of time and state, facilitating the analysis.

Subsequently, the state process $\{X_t\}_{t\in[0,T]}$ is defined as:

$$X_t := \varepsilon_t - \int_0^t r_s(A_s)\, ds, \quad t \in [0, T]. \tag{24}$$

Assuming that the martingale $\varepsilon_t = \mathbb{E}^{\mathbb{Q}}(\varepsilon_T \mid \mathcal{F}_t)$, for $t \in [0, T]$, is modeled using a general jump-diffusion process adapted to the filtration, the state process $\{X_t\}_{t\in[0,T]}$ is the solution of the stochastic differential equation:

$$dX_t = -r(\alpha(t, X_t))\, dt + \sigma(t, X_t)\, dW_t + \int_{\mathbb{R}\setminus\{0\}} a(t-, X_{t-}, y)\, (p_v - q_v)(dy \times dt), \tag{25}$$

where $\{W_t\}_{t\in[0,T]}$ is a Brownian motion adapted to the filtration $\{\mathcal{F}_t\}_{t\in[0,T]}$, and p_v is a random Poisson measure independent of $\{W_t\}_{t\in[0,T]}$ and $\{\mathcal{F}_t\}_{t\in[0,T]}$, with intensity $q_v(dy \times dt) = \lambda v(dy)\, dt$. Here, v is a probability distribution on $\mathbb{R}$, $\lambda \geq 0$ is a positive constant, and the impact of jumps is incorporated through the function a, which describes the average jump size. Note that $\nu(dy) := \lambda v(dy)$ is the Lévy measure of the jump-diffusion model.

To ensure the martingale property of the allowance price process, we will apply the Itô's formula to derive the stochastic differential of the process and then we are going to wipe out the drift term. But, first, let us introduce the Itô's formula and the Itô table, presented in [11]:

Itô Table

$\times$	$dW(t)$	dt
$dW(t)$	dt	0
dt	0	0

Theorem 1: Itô's Formula

Let X_t be an Itô process defined by $X_t = X_a + \int_a^t f(s)\, dW(s) + \int_a^t g(s)\, ds$, and let $h(t, x)$ be a continuous function with continuous partial derivatives $\partial_{(1,0)}h$, $\partial_{(0,1)}h$, and $\partial_{(0,2)}h$, where $\partial_{(i,j)}$ denotes the partial derivative of order i with respect to the time variable and of order j with respect to the space variable.

Then $h(t, X_t)$ is an Itô process, and:

$$h(t, X_t) = h(a, X_a) + \int_a^t \partial_{(0,1)}h(s, X_s) f(s)\, dW(s) +$$

$$+ \int_a^t \left[\partial_{(1,0)}h(s, X_s) + \partial_{(0,1)}h(s, X_s) g(s) + \frac{1}{2}\partial_{(0,2)}h(s, X_s) f(s)^2 \right] ds.$$

The proof of this result is omitted, as it lies beyond the scope of this project. There exists a formal analogy between Itô's formula and the second-order Taylor formula. More precisely, considering the Itô table, Itô's formula can be expressed as:

$$dh(t,X_t) = \partial_{(1,0)}h(t,X_t)\,dt + \partial_{(0,1)}h(t,X_t)\,dX_t + \frac{1}{2}\partial_{(2,0)}h(t,X_t)(dt)^2 +$$

$$+\frac{1}{2}\partial_{(0,2)}h(t,X_t)(dX_t)^2 + \partial_{(1,1)}h(t,X_t)(dt)(dX_t).$$

Applying the Itô table, this simplifies to:

$$dh(t,X_t) = \partial_{(1,0)}h(t,X_t)\,dt + \partial_{(0,1)}h(t,X_t)\,dX_t + \frac{1}{2}\partial_{(0,2)}h(t,X_t)(dX_t)^2. \tag{26}$$

To have a better understanding of how to use the Itô table and the Itô formula, the formula will be applied, in the Appendix A, to the process $A_t = \alpha(t, X_t)$, where X_t is a particular Itô Process and we will see that if we require A_t to be a martingale then we can derive a partial differential equation for α.

Let us now introduce a general jump-diffusion process as the process

$$X_t = X_0 + \int_0^t f(s)dWs + \int_0^t g(s)ds + \int_0^t \int_{\mathbb{R}\setminus\{0\}} l(s,y)(p_v - q_v)(dy \times ds) \tag{27}$$

where f and g satisfy the same assumptions as in an Itô Process and l is a process such that the stochastic integral $\int_0^t \int_{\mathbb{R}\setminus\{0\}} l(s,y)(p_v - q_v)(dy \times ds)$ is well defined (see the detailed conditions in section 4.2 of [13]).

Let us also denote the continuous part of X_t by

$$X_t^c = X_0 + \int_0^t f(s)dWs + \int_0^t g(s)ds \tag{28}$$

Then we can write the Itô Formula for the general jump-diffusion process when $h(t,x)$ is a $C^{1,2}$ function by:

$$dh(t,X_t) = \partial_{(1,0)}h(t,X_{t-})\,dt + \partial_{(0,1)}h(t,X_{t-})\,dX_t^c + \frac{1}{2}\partial_{(0,2)}h(t,X_{t-})(dX_t^c)^2$$

$$+\int_0^t \int_{\mathbb{R}\setminus\{0\}} \left[h(t,X_{t-} + l(t,y)) - h(t,X_{t-})\right](p_v - q_v)(dy \times dt)$$

$$+\int_{\mathbb{R}\setminus\{0\}} \left[h(t,X_{t-} + l(t,y)) - h(t,X_{t-}) - l(t,y)\partial_{(0,1)}h(t;X_{t-})\right] q_v(dy \times dt).$$

Note that the Itô Formula in Theorem 1 is a particular case of this more general Itô Formula.

For a proof of the Itô Formula for general jump-diffusion process and Lévy Processes see section 4.4 of [13] or section 8.3 of [6].

Applying this Itô Formula to $A_t = \alpha(t, X_t)$, for $t \in [0,T]$, and considering that X_t is the solution of the stochastic differential equation (SDE)

$$dX_t = -r(\alpha(t,X_{t-}))dt + \sigma(t,X_{t-})dW_t + \int_{\mathbb{R}\setminus\{0\}} a(t-,X_{t-},y)(p_v - q_v)(dy \times dt), \tag{29}$$

we obtain

$$d\alpha(t,X_t) = \partial_{(1,0)}\alpha(t,X_{t-})dt + \partial_{(0,1)}\alpha(t,X_{t-})[-r(\alpha(t,X_{t-}))dt + \sigma(t,X_{t-})dW_t)]$$
$$+\frac{1}{2}\sigma^2(t,X_{t-})\partial_{(0,2)}\alpha(t,X_{t-})dt + \int_{\mathbb{R}\setminus\{0\}} [\alpha(t,X_{t-}+a(t-,X_{t-},y)) - \alpha(t,X_{t-})]\,(p_v - q_v)(dy\times dt) +$$
$$+\int_{\mathbb{R}\setminus\{0\}} \left[\alpha(t,X_{t-}+a(t-,X_{t-},y)) - \alpha(t,X_{t-}) - a(t-,X_{t-},y)\partial_{(0,1)}\alpha(t,X_{t-})\right] q_v(dy\times dt)$$

If we require that $A_t = \alpha(t,X_t)$ is a martingale, then the drift component of $d\alpha(t,X_t)$ must be zero. Therefore,

$$\partial_{(1,0)}\alpha(t,X_{t-}) - r(\alpha(t,X_{t-}))\partial_{(0,1)}\alpha(t,X_{t-}) + \frac{1}{2}\sigma^2(t,X_{t-})\partial_{(0,2)}\alpha(t,X_{t-}) +$$
$$\int_{\mathbb{R}\setminus\{0\}} \left[\alpha(t,X_{t-}+a(t-,X_{t-},y)) - \alpha(t,X_{t-}) - a(t-,X_{t-},y)\partial_{(0,1)}\alpha(t,X_{t-})\right] \lambda v(dy)dt = 0.$$

Introducing the function $\beta(\tau,x) := \alpha(T-t,x)$, replacing X_{t-} by x and considering that the function $a(t,x,y)$ is continuous, the previous equation transforms into the nonlinear partial integro-differential equation for β:

$$\begin{aligned}\partial_{(1,0)}\beta(\tau,x) = -r(\beta(\tau,x))\partial_{(0,1)}\beta(\tau,x) + \frac{1}{2}\sigma^2(\tau,x)\partial_{(0,2)}\beta(\tau,x)\\ + \lambda\int \left[\beta(\tau,x+a(\tau,x,y)) - \beta(\tau,x) - a(\tau,x,y)\partial_{(0,1)}\beta(\tau,x)\right]v(dy) = 0,\end{aligned} \tag{30}$$

where $(\tau,x)\in[0,T]\times\mathbb{R}$, subject to the boundary condition:

$$\beta(0,x) = \pi\mathbb{1}(x\geq 0), \quad x\in\mathbb{R}.$$

Consult [12] to see the conditions that ensure that the stochastic differential equation possesses a unique strong solution.

Assuming there exists a classical solution $\beta\in C^{1,2}([0,T]\times\mathbb{R})$ for the problem defined by the previous equations, if this solution satisfies the maximum principle, then:

$$0\leq\beta(\tau,x)\leq\pi, \quad (\tau,x)\in[0,T]\times\mathbb{R}.$$

This implies that the certificate price remains within realistic physical bounds:

- The lowest possible value is zero (in the case of an excess of certificates).
- The highest possible value is π (the maximum penalty in the case of a shortage).

If β is a classical solution of (30), then A_t will be a local martingale. Thus, if the solution $\beta(\tau,x)$ satisfies the maximum principle, the local martingale $A_t = \alpha(t,X_t)$ is bounded, Therefore is a martingale under the risk-neutral measure $\mathbb{Q}$.

Let us prove that the solution $\beta(\tau,x)$ indeed satisfies the maximum principle.

Proposition 2:

Assuming that $\beta(\tau,x)$ is a classical solution to equation (30) with the initial boundary condition $\beta(0,x)=h(x)$, then $\beta(\tau,x)$ satisfies the maximum principle:

$$\inf_z h(z)\leq\beta(\tau,x)\leq\sup_z h(z), \quad (\tau,x)\in[0,T]\times\mathbb{R}. \tag{31}$$

Proof. To prove that $\beta(\tau, x)$ satisfies the maximum principle, we utilize the relationship between $\alpha(t, x)$ and $\beta(\tau, x)$:

$$\alpha(t, x) = \beta(T - t, x).$$

Since $\beta(\tau, x)$ satisfies the equation (30), the certificate price $A_t = \alpha(t, X_t)$ is a martingale under $\mathbb{Q}$. Additionally, the process $\{X_t\}$ is Markovian, which implies:

$$\alpha(t, X_t) = \mathbb{E}(A_T \mid \mathcal{F}_t) = \mathbb{E}(\alpha(T, X_T) \mid X_t).$$

Due to the regularity of $\alpha(t, x)$, for $\tau = T - t$, we have:

$$\beta(\tau, x) = \alpha(t, x) = \mathbb{E}(\alpha(T, X_T) \mid X_t = x) = \mathbb{E}(\beta(0, X_T) \mid X_t = x) = \mathbb{E}(h(X_T) \mid X_t = x).$$

Therefore, the expected value of $h(X_T)$ is bounded by the minimum and maximum values of $h(z)$, which directly implies the maximum principle:

$$\inf_z h(z) \leq \beta(\tau, x) \leq \sup_z h(z).$$

□

Finally, we are ready to proceed with the discretization.

3.3 Numerical Discretization

In the mathematical modeling of emission markets, the nonlinear partial integro-differential equation (PIDE) described in Equation (30) is fundamental for capturing the evolution of emission certificate prices. However, as noted in the article [5], analytical solutions for partial integro-differential equations are rare and limited to special cases. In most practical scenarios, it becomes necessary to employ numerical methods to solve these equations.

Discretizing the PIDE is a critical step in transforming the continuous problem into a system of finite difference equations that can be solved numerically. In this section, we will discuss how to discretize Equation (30) using the finite difference method and demonstrate that the discretized problem admits a unique solution, following the procedures described in [5], [14] and [15]

First, we will present some definitions and the discretization grid.

1. **Spatial Domain Truncation:**

   To simplify the problem, we truncate the spatial domain of x. We define:

   $$D_l := \{x \in \mathbb{R} : |x| < l\}, \tag{32}$$

   where $l > 0$ is chosen such that the probability of the process $\{X_t\}$ exiting the domain D_l during the time interval $[0, T]$, given it starts at X_0, does not exceed a small value ϵ. See [5] to have a method for choosing the domain boundary l.

2. **Integration Domain Restriction:**

   The integral on the right-hand side of Equation (30) is restricted to an interval $[K_1, K_2]$, selected to ensure that the error introduced by this truncation remains minimal. For an optimal choice of the endpoints K_j, refer to the study presented in [14].

3. **Discrete Grid:**

   The numerical solution will be computed on a discrete grid. Let N be the total number of discrete x-values and M the total number of τ-values to be used in the grid for the numerical solution. The step sizes in x and τ are respectively $\Delta_x = 2l/N$ and $\Delta_\tau = T/M$. Then the grid will be defined as:

$$x_i = -l + i\Delta_x, \quad \tau_n = n \cdot \Delta_\tau, \quad \text{for} \quad i \in \mathbb{Z} \quad \text{and} \quad n = 0, \dots, M.$$

Discretization

Let $\beta_i^n = \beta(\tau_n, x_i)$ denote the values of β on the grid. Due to the nonlocal term on the right-hand side of Equation (30), we need to define β outside the domain $[0,T] \times D_l$. We adopt the simplest and most intuitive approach by setting:

$$\beta_i^n := g(x_i) \quad \text{for} \quad i \notin \{0, \dots, N-1\},$$

where

$$g(x) := \begin{cases} \pi & \text{if } x \geq l, \\ 0 & \text{if } x \leq -l. \end{cases}$$

To approximate the partial derivatives, it will be used the first order finite differences, which are used to approximate the first order derivative of a function f.

Forward Difference

The forward difference of f is defined as

$$f'(x) = \frac{f(x+h) - f(x)}{h}. \tag{33}$$

Central Difference

The central difference of f is defined as

$$f'(x) = \frac{f(x+h) - f(x-h)}{2h}. \tag{34}$$

Backward Difference

The backward difference of f is defined as

$$f'(x) = \frac{f(x) - f(x-h)}{h}. \tag{35}$$

Thus, the partial derivatives are approximated using the following finite difference formulas:

- **Temporal Derivative**

  The partial temporal derivative is approximated by the forward finite difference:

$$\partial_{(1,0)}\beta(\tau_n, x_i) \approx \frac{\beta(\tau_{n+1}, x_i) - \beta(\tau_n, x_i)}{\Delta_\tau} = \frac{\beta_i^{n+1} - \beta_i^n}{\Delta_\tau} \tag{36}$$

- **Spatial Derivative**

  The partial spatial derivative is approximated by the backward finite difference:

$$\partial_{(0,1)}\beta(\tau_n, x_i) \approx \frac{\beta(\tau_n, x_i) - \beta(\tau_n, x_{i-1})}{\Delta_x} = \frac{\beta_i^n - \beta_{i-1}^n}{\Delta_x} \tag{37}$$

- **Second Spatial Derivative**

  The second partial spatial derivative is approximated by the second order central finite difference:

$$\partial_{(0,2)}\beta(\tau_n, x_i) \approx \frac{\beta(\tau_n, x_{i+1}) - 2\beta(\tau_n, x_i) + \beta(\tau_n, x_{i-1})}{(\Delta_x)^2} = \frac{\beta_{i+1}^n - 2\beta_i^n + \beta_{i-1}^n}{(\Delta_x)^2} \tag{38}$$

To discretize the integral term

$$\lambda \int_{\mathbb{R}\setminus\{0\}} \beta(\tau_n, x_i + a(\tau_n, x_i, y))\, v(dy), \tag{39}$$

we adopt a strategy similar to that in [15]. To this end, we use the same step size Δ_x to approximate the integral term and select J_1 and J_2 such that

$$[K_1, K_2] \subseteq \left[(J_1 - \frac{1}{2})\Delta_x, (J_2 + \frac{1}{2})\Delta_x\right], \tag{40}$$

and define, for each subinterval $\left[(j - \frac{1}{2})\Delta_x, (j + \frac{1}{2})\Delta_x\right]$, where $j = J_1, \ldots, J_2$,

$$v_j := \int_{j-(1/2)\Delta_x}^{j+(1/2)\Delta_x} v(dy). \tag{41}$$

Then, by choosing the index

$$j^*(i, j, n) = \arg\min_k |x_i + a(\tau_n, x_i, x_j) - (k\Delta_x - l)| \tag{42}$$

to minimize the distance between the point $x_i + a(\tau_n, x_i, x_j)$ and the center of the corresponding subinterval, the integral term can be approximated by

$$\lambda \int_{\mathbb{R}\setminus\{0\}} \beta(\tau_n, x_i + a(\tau_n, x_i, y))\, v(dy) \approx \lambda \sum_{j=J_1}^{J_2} v_j \beta_{j^*(i,j,n)}^n. \tag{43}$$

The same approach can be applied to the integral term

$$\partial_{(0,1)}\beta(\tau_n, x_i) \int_{K_1}^{K_2} a(\tau_n, x_i, y) v(dy) \approx \frac{\beta_i^n - \beta_{i-1}^n}{\Delta x} \sum_{j=0}^{N} a_{i,j}^n v_j, \tag{44}$$

where $a_{i,j}^n := a(\tau_n, x_i, x_j)$.

For simplification, let us define

$$\Sigma_i^n := \sum_{j=0}^{N} a_{i,j}^n v_j.$$

Substituting all the terms into Equation (30), the objective becomes to find a solution β_i^n on the grid such that:

$$\frac{\beta_i^{n+1}-\beta_i^n}{\Delta_\tau} = \frac{1}{2}\sigma^2(\tau_{n+1},x_i)\frac{\beta_{i+1}^{n+1}-2\beta_i^{n+1}+\beta_{i-1}^{n+1}}{(\Delta_x)^2} - r(\beta_i^n)\frac{\beta_i^{n+1}-\beta_{i-1}^{n+1}}{\Delta_x}$$
$$+\lambda\sum_{j=J_l}^{J_r} v_j\beta_{j^*(i,j,n)}^n - \lambda\beta_i^{n+1} - \lambda\frac{\beta_i^{n+1}-\beta_{i-1}^{n+1}}{\Delta_x}\Sigma_i^{n+1}, \tag{45}$$

with the initial and boundary conditions:

$$\beta_i^0 = \pi\mathbf{1}(x_i \geq 0) \quad \text{for} \quad i \in \mathbb{Z}, \quad \beta_i^n = g(x_i) \quad \text{for} \quad i < 0 \quad \text{and} \quad i \geq N.$$

To complete the theoretical framework, it is necessary to finally ensure that the discretized solution exists, is unique, and satisfies the maximum principle. If these conditions are met, the process $A_t = \alpha(t, X_t)$ will be a martingale under the risk-neutral measure $\mathbb{Q}$. Consequently, the task of determining the $\mathbb{Q}$-martingale $\{A_t^*\}_{t=0}^{T-1}$ such that the terminal price satisfies:

$$A_T^* = \pi\mathbb{1}\left(\varepsilon_T - \sum_{t=0}^{T-1} r_t(A_t^*) \geq 0\right),$$

will be successfully accomplished.

To address this, we present the following proposition.

Proposition 3:

The discretized problem (45) admits a unique solution $\{\beta_i^n\}$. Furthermore, defining:

$$\Sigma^* := \min \Sigma_i^n \quad \text{and} \quad \sigma^{*2} := \min \sigma^2(\tau_n, x_i),$$

where the minima are taken over all $i \in \{0, \dots, N-1\}$ and $n \in \{0, \dots, M\}$, if σ^2 is bounded away from zero and the discrete grid satisfies the condition

$$-\Sigma^*\Delta_x \leq \frac{\sigma^{*2}}{2\lambda}, \tag{46}$$

then the solution adheres to the maximum principle

$$0 \leq \beta_i^n \leq \pi \quad \text{for all} \quad i \in \mathbb{Z} \quad \text{and} \quad n \in \{0, \dots, M-1\},$$

where π represents the penalty per unit of pollutant not covered by the initial allocation.

This proposition ensures that the discretized problem is well-posed. This implies that:

- The solution exists and is unique.
- Allowance price Process is always non-negative ($\beta_i^n \geq 0$).
- Allowance price Process never exceed the penalty level set by the regulator ($\beta_i^n \leq \pi$).

This is crucial as it reflects the realistic physical conditions of the emission certificate market. The proposition was proved in [5]. We present a more detailed version of the proof in order to clarify the original proof.

Proof. We begin by showing that the discretized equation can be rewritten, for $i \in \{0, \ldots, N-1\}$ and $n \in \{0, \ldots, M-1\}$, as

$$-F_i^n(\beta_i^n)\Delta_\tau \beta_{i-1}^{n+1} + (1 + G_i^n(\beta_i^n)\Delta_\tau)\beta_i^{n+1} - H_i^n \Delta_\tau \beta_{i+1}^{n+1} = \beta_i^n + \lambda \Delta_\tau \sum_{j=J_l}^{J_r} v_j \beta_{j^*(i,j,n)}^n, \tag{47}$$

where

$$\begin{aligned}
F_i^n(\beta_i^n) &= \frac{\sigma^2(\tau_{n+1}, x_i)}{2(\Delta_x)^2} + \frac{r(\beta_i^n)}{\Delta_x} \frac{\lambda \Sigma_i^{n+1}}{\Delta_x}, \\
G_i^n(\beta_i^n) &= \frac{\sigma^2(\tau_{n+1}, x_i)}{(\Delta_x)^2} + \frac{r(\beta_i^n)}{\Delta_x} + \frac{\lambda \Sigma_i^{n+1}}{\Delta_x} + \lambda, \\
H_i^n &= \frac{\sigma^2(\tau_{n+1}, x_i)}{2(\Delta_x)^2}.
\end{aligned}$$

Rearranging the terms involving β_i^{n+1}, β_i^n, and β_i^{n+1}, we have:

$$\begin{aligned}
\frac{\beta_i^{n+1} - \beta_i^n}{\Delta_\tau} &= \frac{1}{2}\sigma^2(\tau_{n+1}, x_i) \frac{\beta_{i+1}^{n+1} - 2\beta_i^{n+1} + \beta_{i-1}^{n+1}}{(\Delta_x)^2} - r(\beta_i^n) \frac{\beta_i^{n+1} - \beta_{i-1}^{n+1}}{\Delta_x} \\
&\quad + \lambda \sum_{j=J_l}^{J_r} v_j \beta_{j^*(i,j,n)}^n - \lambda \beta_i^{n+1} - \lambda \frac{\beta_i^{n+1} - \beta_{i-1}^{n+1}}{\Delta_x} \Sigma_i^{n+1} = \\
\frac{\beta_i^{n+1} - \beta_i^n}{\Delta_\tau} &= \left(\frac{1}{2}\sigma^2(\tau_{n+1}, x_i) \frac{1}{(\Delta_x)^2} + r(\beta_i^n) \frac{1}{\Delta_x} + \lambda \Sigma_i^{n+1} \frac{1}{\Delta_x} \right) \beta_{i-1}^{n+1} \\
&\quad + \left(\frac{1}{2}\sigma^2(\tau_{n+1}, x_i) \frac{-2}{(\Delta_x)^2} - r(\beta_i^n) \frac{1}{\Delta_x} - \lambda \Sigma_i^{n+1} \frac{1}{\Delta_x} - \lambda \right) \beta_i^{n+1} \\
&\quad + \left(\frac{1}{2}\sigma^2(\tau_{n+1}, x_i) \frac{1}{(\Delta_x)^2} \right) \beta_{i+1}^{n+1} + \lambda \sum_{j=J_l}^{J_r} v_j \beta_{j^*(i,j,n)}^n.
\end{aligned}$$

Multiplying both sides of the equation by Δ_τ and adding β_i^n, the above equation can be rewritten as:

$$\begin{aligned}
&- \left(\frac{1}{2}\sigma^2(\tau_{n+1}, x_i) \frac{1}{(\Delta_x)^2} + r(\beta_i^n) \frac{1}{\Delta_x} + \lambda \Sigma_i^{n+1} \frac{1}{\Delta_x} \right) \Delta_\tau \beta_{i-1}^{n+1} \\
&+ \left(1 + \left(\frac{1}{2}\sigma^2(\tau_{n+1}, x_i) \frac{2}{(\Delta_x)^2} + r(\beta_i^n) \frac{1}{\Delta_x} + \lambda \Sigma_i^{n+1} \frac{1}{\Delta_x} + \lambda \right) \Delta_\tau \right) \beta_i^{n+1} \\
&- \left(\frac{1}{2}\sigma^2(\tau_{n+1}, x_i) \frac{1}{(\Delta_x)^2} \right) \Delta_\tau \beta_{i+1}^{n+1} = \lambda \Delta_\tau \sum_{j=J_l}^{J_r} v_j \beta_{j^*(i,j,n)}^n + \beta_i^n.
\end{aligned}$$

Thus, if we define $F_i^n(\beta_i^n)$, $G_i^n(\beta_i^n)$, and H_i^n as described above, we arrive at Equation (47), as intended to demonstrate.

This equation represents a linear system that can be expressed in matrix form:

$$M(n)\beta^{n+1} = \gamma_n \quad \text{for all} \quad n = 0, \ldots, M-1, \tag{48}$$

where $\beta^{n+1} = (\beta_0^{n+1}, \ldots, \beta_{N-1}^{n+1}) \in \mathbb{R}^N$, $\gamma_n = (\gamma_0^n, \ldots, \gamma_{N-1}^n) \in \mathbb{R}^N$ with components

$$\gamma_i^n = \beta_i^n + \lambda\Delta_\tau \sum_{j=J_l}^{J_r} v_j \beta_{j^*(i,j,n)}^n, \quad i = 0, \ldots, N-2,$$

and

$$\gamma_{N-1}^n = \beta_{N-1}^n + \lambda\Delta_\tau \sum_{j=J_l}^{J_r} v_j \beta_{j^*(N-1,j,n)}^n + H_{N-1}^n \Delta_\tau \pi.$$

This matrix $M(n) \in \mathbb{R}^{N\times N}$ is tridiagonal, with the following structure:

- Elements above the main diagonal: $-H_i^n \Delta\tau$,
- Elements on the main diagonal: $1 + G_i^n(\beta^n)\Delta\tau$,
- Elements below the main diagonal: $-F_i^n(\beta^n)\Delta\tau$.

Furthermore, it is worth noting the following relationship:

$$G_i^n(\beta_i^n) = F_i^n(\beta_i^n) + H_i^n + \lambda \iff |1 + G_i^n(\beta_i^n)\Delta_\tau| > |-F_i^n(\beta_i^n)\Delta_\tau| + |-H_i^n\Delta_\tau|$$

for $\quad i = 0, \ldots, N-1 \quad$ and $\quad n = 0, \ldots, M.$

This relationship ensures that $M(n) \in \mathbb{R}^{N\times N}$ is diagonally dominant with non-negative coefficients. Since it is strictly diagonally dominant, the matrix is invertible, which in turn implies that the solution β_i^{n+1} is unique (see [16]). Consequently, the existence and uniqueness of the solution to the discretized equation follow by induction.

To complete the proof of Proposition 3, it remains to demonstrate that the maximum principle holds. To this end, it will be prove that β_i^n are non-negative, as the argument can be readily adapted to show that the values β_i^n remain bounded by π.

We will use mathematical induction to prove this:

- **Base Case ($n = 0$):** The boundary condition $\beta(0, x) = \pi\mathbf{1}_{(x\geq 0)}$ and the definition of $g(x)$ ensure that $\beta_i^0 \geq 0$ for all $i \in \mathbb{Z}$.
- **Inductive Hypothesis:** Assume that $\beta_i^n \geq 0$ for all $i \in \mathbb{Z}$.

Inductive Step: Suppose, for the sake of contradiction, that there exists some $i_0 \in \mathbb{Z}$ such that $\beta_{i_0}^{n+1} < 0$. Given that the function $g \geq 0$ by definition, it follows that $i_0 \in \{0, \ldots, N-1\}$. Choose i_0 such that:

$$\beta_{i_0}^{n+1} = \min_{i\in\{0,\ldots,N-1\}} \beta_i^{n+1} < 0.$$

Since the functions F_i^n, G_i^n, and H_i^n are all non-negative, and given the relationship

$$G_i^n(\beta_i^n) = F_i^n(\beta_i^n) + H_i^n + \lambda,$$

we have

$$G_i^n(\beta_{i_0}^n) - F_i^n(\beta_{i_0}^n) - H_i^n - \lambda = 0 \iff G_i^n(\beta_{i_0}^n)\Delta_\tau - F_i^n(\beta_{i_0}^n)\Delta_\tau - H_i^n\Delta_\tau - \lambda = 0 \iff$$
$$\beta_{i_0}^{n+1} = (1 + G_i^n(\beta_{i_0}^n)\Delta_\tau)\beta_{i_0}^{n+1} - F_i^n(\beta_{i_0}^n)\Delta_\tau\beta_{i_0}^{n+1} - H_i^n\Delta_\tau\beta_{i_0}^{n+1} - \lambda\Delta_\tau\beta_{i_0}^{n+1}.$$

Since the term $-\lambda \Delta_\tau \beta_{i_0}^{n+1} \geq 0$ (because $\beta_{i_0}^{n+1} < 0$ and $\lambda, \Delta_\tau > 0$), it follows that:

$$\beta_{i_0}^{n+1} \geq (1 + G_i^n(\beta_{i_0}^n)\Delta_\tau)\beta_{i_0}^{n+1} - F_i^n(\beta_{i_0}^n)\Delta_\tau \beta_{i_0}^{n+1} - H_i^n \Delta_\tau \beta_{i_0}^{n+1}.$$

Given that

$$\beta_{i_0}^{n+1} = \min_{i \in \{0,\ldots,N-1\}} \beta_i^{n+1} < 0,$$

we can deduce:

- $-F_i^n(\beta_{i_0}^n)\Delta_\tau \beta_{i_0}^{n+1} \geq -F_i^n(\beta_{i_0}^n)\Delta_\tau \beta_{i_0-1}^{n+1}$ because $\beta_{i_0}^{n+1} \leq \beta_{i_0-1}^{n+1}$,
- $-H_i^n \Delta_\tau \beta_{i_0}^{n+1} \geq -H_i^n \Delta_\tau \beta_{i_0+1}^{n+1}$ because $\beta_{i_0}^{n+1} \leq \beta_{i_0+1}^{n+1}$.

Thus, we can conclude that

$$\beta_{i_0}^{n+1} \geq (1 + G_i^n(\beta_{i_0}^n)\Delta_\tau)\beta_{i_0}^{n+1} - F_i^n(\beta_{i_0}^n)\Delta_\tau \beta_{i_0}^{n+1} - H_i^n \Delta_\tau \beta_{i_0}^{n+1}$$

$$\geq (1 + G_i^n(\beta_{i_0}^n)\Delta_\tau)\beta_{i_0-1}^{n+1} - F_i^n(\beta_{i_0}^n)\Delta_\tau \beta_{i_0+1}^{n+1} - H_i^n \Delta_\tau \beta_{i_0+1}^{n+1} = \beta_{i_0}^n + \lambda \Delta_\tau \sum_{j=J_l}^{J_r} v_j \beta_{j^*(i,j,n)}^n,$$

where the last step follows directly from Equation (47). By the inductive hypothesis, we have

$$\beta_{i_0}^n + \lambda \Delta_\tau \sum_{j=J_l}^{J_r} v_j \beta_{j^*(i,j,n)}^n \geq 0 \implies \beta_{i_0}^{n+1} \geq 0,$$

which contradicts our initial assumption. Therefore, the proposition is proved. □

In this section, we have developed a theoretical model to describe the dynamics of emission certificate prices within the context of jumps and diffusion, accounting for information shocks that abruptly influence market agents expectations. The proposed model is based on a nonlinear partial integro-differential equation (PIDE), which integrates both continuous components (diffusion) and discontinuities (jumps). We have demonstrated that this equation can be solved numerically and, furthermore, established the existence and uniqueness of the discretized solution, while also validating the maximum principle. This ensures that the simulated prices remain within realistic bounds (between zero and the penalty value).

With this foundation, we are now prepared to proceed with the numerical results.

4 Results

In this section, we present the numerical results obtained from the implementation of the jump-diffusion model for emission certificate prices. The objective is to empirically validate the theoretical properties developed earlier and to demonstrate the practical applicability of the model in pricing derivatives related to the emissions market. A stable and efficient finite difference scheme was employed to numerically solve the nonlinear partial integro-differential equation governing the certificate price process, incorporating both continuous components (diffusion) and discontinuities (jumps). The results, will be given to different distributions for the jumps and will include an analysis of the temporal evolution of certificate prices across various parametric scenarios, as well as an assessment of the error arising from spatial truncation. **Parameters Utilized:**

First, we will present the parameters that were adopted:

1. **Time Unit:** We consider a time unit equivalent to 1 year, setting the compliance horizon as $T = 1$.

2. **Diffusion Function:** For simplicity, we assume a constant diffusion function $\sigma(t, x) = \sigma$, where $\sigma = 1$.

3. **Compound Poisson Process:** In the beginning, the jump process will be modeled using a standard normal distribution $v = \mathcal{N}(0, 1)$, with an intensity rate $\lambda = 1$.

4. **Cumulative Reduction Function:** We adopt a linear cumulative reduction function $r(a) = a$ for all $a \in [0, \pi]$.

5. **Penalty Level:** The penalty level is fixed at $\pi = 1$.

6. **Spatial Domain Truncation:** To manage errors from spatial truncation, we selected a maximum tolerable error $\epsilon_1 = \epsilon_2 = 0.05$, resulting in a boundary limit $l \approx 11$ (see [5], [17], [18] for more information on how this was done).

7. **Function a :** We focus on a special case where $a(\tau, x, y) = y$ holds for all $y \in \mathbb{R}$.

8. **Time Step:** $\Delta_t = 0.02$, which implies the following number of temporal points

$$M = \frac{T}{\Delta_t} = \frac{1}{0.02} = 50. \tag{49}$$

9. **Space Step:** $\Delta_x = 0.02$, which implies the following number of spacial points

$$N = \frac{2l}{\Delta_x} = \frac{2l}{0.02} = 100l. \tag{50}$$

4.1 Truncation Error

The control of truncation error is crucial to guarantee the reliability of numerical results. To this end, we consider the L_1 norm of the difference between two solutions $\beta^n(l)$ and $\beta^n(\tilde{l})$, corresponding to the truncation limits $\pm l$ and $\pm\tilde{l}$, respectively:

$$\sum_i \sum_{n=0}^{M} \left| \beta_i^n(l) - \beta_i^n(\tilde{l}) \right|, \quad l < \tilde{l}, \tag{51}$$

where the sum is performed over all points in the fixed sub-region $[0, T] \times [-d, d]$ with $d < l < \tilde{l}$. Numerical experiments demonstrate that, for $d = 11$, $l = 20$, $\tilde{l} = 30$, the error is of the order 10^{-8}. This allows us to conclude that the solution $\{\beta_i^n\}$ calculated over the spatial region $[-30, 30]$ is highly accurate.

4.2 Normal Distribution

The selection of a standard normal distribution to model jumps in the context of emission certificate prices is a natural and well-justified choice, rooted in both financial and environmental perspectives. This approach offers several advantages that support its use in stochastic jump-diffusion models, particularly in environments characterized by incomplete information or sudden shocks.

This distribution is symmetric around a mean of zero, enabling a balanced representation of both positive and negative events. In the context of emissions markets, this allows the model to capture unforeseen shocks that may drive certificate prices upward (e.g., a sudden surge in demand for credits) or downward (e.g., the unexpected emergence of new emission reduction technologies). Although the tails of a normal distribution are not as heavy as those of some alternative distributions, they still provide a reasonable approximation for moderate extreme events, which are commonly observed in market settings. Moreover, the standard normal distribution offers a clear interpretation of its parameters: a mean of zero reflects the absence of a systematic trend in jumps, while the unit variance (or an adjusted variance) governs the magnitude of volatility induced by these shocks.

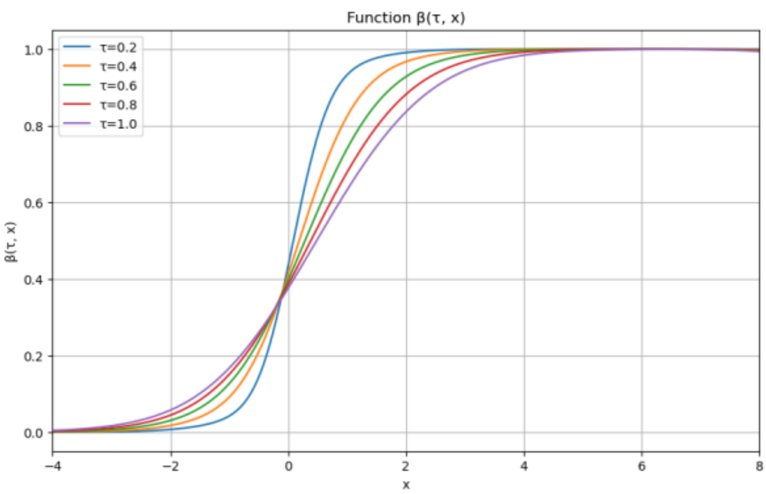

Figure 1: Plot of the function $\alpha(t, .)$ for $t = 0, 0.2, 0.4, 0.6, 0.8$ calculated by discretization (45) with parameters given in the text.

Figure 1 illustrates the function $\alpha(t, \cdot)$, which represents the emission certificate price (allowance price) as a function of the state x for various times $t = 0, 0.2, 0.4, 0.6, 0.8$. Since $\alpha(t, x) = \beta(T - t, x)$, where $\tau = T - t$ denotes the time to maturity, the graph reflects the evolution of the certificate price as it approaches the maturity date ($t = T$). Additionally, it indicates that $\alpha(t, x)$ is a smooth, monotonically increasing function of x, varying between 0 and π (the penalty level, set to $\pi = 1$ in the numerical example). This aligns with the maximum principle (Proposition 3), which ensures that $0 \leq \alpha(t, x) \leq \pi$.

Key observations include:

- The curve for $\tau = 1$ ($t = 0$), representing the start of the compliance period, is the smoothest, reflecting greater uncertainty regarding the future market state (whether there will be a shortage or surplus of certificates).
- The curve for "0.2 to maturity" ($\tau = 0.2$, or $t = 0.8$) is the steepest and closest to the behavior at maturity, where the function α would resemble a step function. So it converges faster than the others toward the boundary condition $\alpha(1, x) = \pi\mathbf{1}(x \geq 0) = 1 \cdot \mathbf{1}(x \geq 0)$.
- As τ decreases (or t increases), the curves for $\tau = 0.8, 0.6, 0.4, 0.2$ (corresponding to $t = 0.2, 0.4, 0.6, 0.8$) become progressively steeper. This indicates that, as maturity approaches, the certificate price converges to the boundary condition $\alpha(1, x) = \pi\mathbf{1}(x \geq 0) = 1 \cdot \mathbf{1}(x \geq 0)$, a step function that is 0 for $x < 0$ (indicating a surplus of certificates) and 1 for $x \geq 0$ (indicating a shortage of certificates).

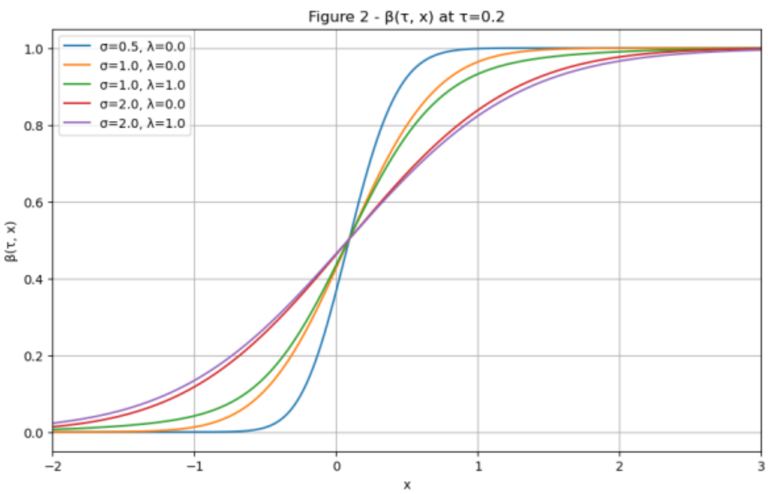

Figure 2: Plot of the function $\alpha(0.8, .)$ for different values of σ and λ.

Figure 2 displays the function $\alpha(0.8, x)$ for varying levels of volatility (σ) and jump intensities (λ), with the aim of illustrating how these parameters influence the emission certificate price at a specific time ($t = 0.8$, or $\tau = T - t = 1 - 0.8 = 0.2$, given $T = 1$).

Dependence on Volatility (σ):

- Figure 2 reveals that, for different values of σ (the volatility of the diffusion component), the function $\alpha(0.8, x)$ exhibits variations in smoothness and slope. When volatility σ is low, the curve becomes steeper, converging more rapidly toward the boundary condition $\alpha(1,x) = \pi\mathbf{1}(x \geq 0) = 1 \cdot \mathbf{1}(x \geq 0)$. This suggests that, with low volatility, market agents anticipate fewer fluctuations, leading to a quicker convergence of the price to 0 (surplus) or $\pi = 1$ (shortage).

- With high σ, the curve is smoother, indicating greater uncertainty due to continuous fluctuations, which delays convergence to the extreme values (0 or π). This reflects the expectation of significant changes in emissions or certificate supply over time.

Impact of Jump Rate (λ):

- The jump rate λ (the intensity of the Poisson process governing jumps) also affects the curve's shape. For higher values of λ, the curve tends to be smoother, as the increased frequency of jumps (discontinuous events, such as regulatory changes or market shocks) heightens uncertainty. This causes the certificate price to take longer to stabilize at 0 or π.
- For low λ, the curve is steeper, suggesting that fewer jump events allow for a more accurate prediction of the market's final state, accelerating convergence toward the boundary condition.

Thus, it can be concluded that for low σ and λ, the curve more closely resembles the step-like shape at maturity, indicating that agents rely on a more predictable price evolution. Conversely, a combination of high volatility (σ large) and high jump rate (λ large) results in smoother curves and slower convergence to extreme values, reflecting greater overall uncertainty in the emissions market.

4.3 Double Exponential Distribution

When analyzing the price behavior of emission certificates using jump-diffusion models, it's important to carefully choose the jump distribution in order to properly reflect the dynamics of the market. To ensure that we have a fair and meaningful comparison across different types of distributions, we need to standardize the expected value ($\mathbb{E}[Y] = 0$) and the variance (Var$(Y) = 1$) of the jumps. This standardization isolates the effects of the distribution's shape, ensuring that differences in variability scale do not confound the analysis. Consequently, by comparing the Standard Normal distribution, characterized by its symmetry and light tails, with the Double Exponential distribution, which incorporates asymmetry and heavy tails, we can directly assess how these properties influence the function $\beta(\tau, x)$ or $\alpha(t, x)$. In this context, adopting the Double Exponential distribution as an alternative for modeling jumps presents a promising approach. Unlike the Standard Normal distribution, the Double Exponential distribution allows for asymmetry in jumps, reflecting market scenarios where events increasing certificate scarcity (upward jumps) or surplus (downward jumps) occur with distinct probabilities and intensities. This feature, combined with its heavy tails, enables the model to better capture rare and impactful events, such as drastic regulatory changes or shocks in fuel demand. To achieve the standardization, the next equalities must hold:

$$\mathbb{E}(Y) = \frac{p}{\eta_1} - \frac{q}{\eta_2} = 0,$$

$$\text{Var}(Y) = pq\left(\frac{1}{\eta_1} + \frac{1}{\eta_2}\right)^2 + \frac{p}{\eta_1^2} + \frac{q}{\eta_2^2} = 1,$$

for $\eta_1 > 1$ and $\eta_2 > 0$.

Consider $p = 0.9$ and $q = 1 - 0.9 = 0.1$. Solving these two equations, we obtain:

$$\eta_1 \approx 1.34161 \quad \text{and} \quad \eta_2 \approx 0.14907.$$

With this parameters, we have the following graphs:

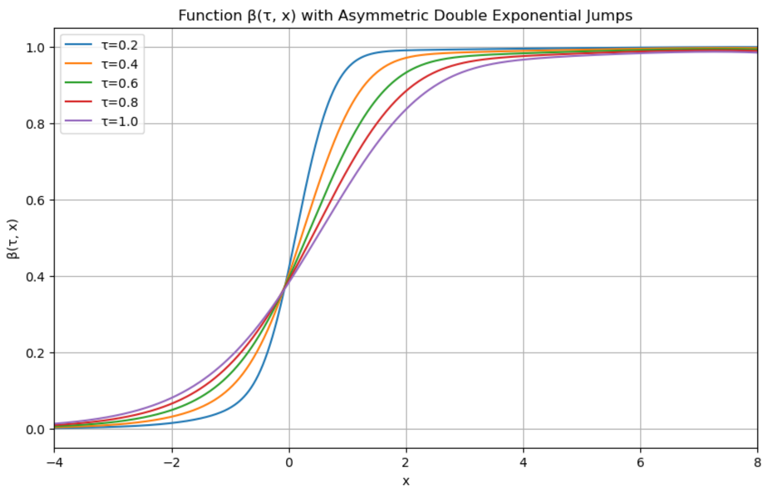

Figure 3: Plot of the function $\alpha(t, .)$ for $t = 0, 0.2, 0.4, 0.6, 0.8$ calculated by discretization (45) with parameters given in the text, but considering a Double Exponential Distribution.

The analysis of the generated graphs, pertaining to the two jump distributions, reveals distinct differences in price dynamics. The symmetric normal distribution produces smooth and balanced $\alpha(t, x)$ curves, reflecting a symmetric dispersion of jumps around zero. In contrast, the asymmetric double exponential distribution results in curves that exhibit a steeper inclination toward higher values as maturity approaches. This trend can be attributed to the higher probability of upward jumps, which increases the frequency of positive shifts in the process X_t, causing the prices A_t to converge more rapidly toward the upper bound π. This reflects a market expectation where events that drive allowance prices, such as stricter regulations or credit shortages, are more probable than events that reduce them. In the reproduced graph, this manifests as curves that rise more quickly or reach higher values near maturity, in comparison to Figure 1, where jumps follow a symmetric normal distribution. Consequently, the choice of an asymmetric distribution may prove more realistic for emissions markets, where events such as new climate policies or energy demand shocks (which tend to elevate prices) occur more frequently than sudden reductions.

To have a more notable difference between the graphs of the function $\alpha(0.8, .)$ for varying values of σ and λ, using a Standard Normal Distribution and a Double Exponential, we will assume that $\lambda \in \{0, 3\}$.

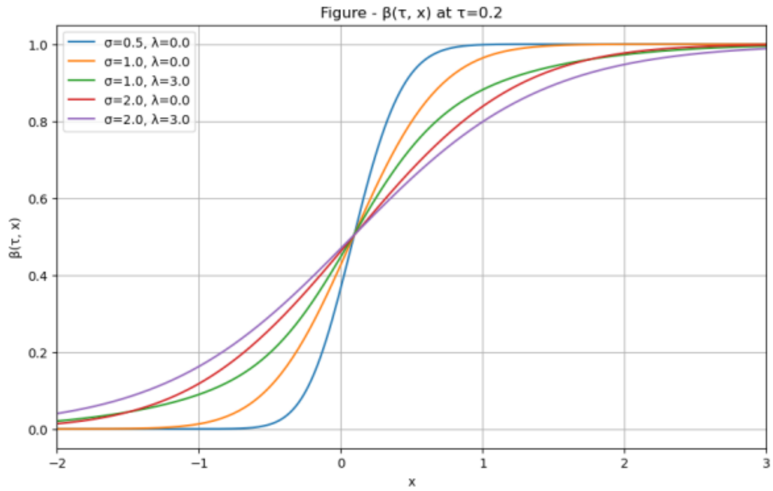

Figure 4: Plot of the function $\alpha(0.8, .)$ for varying values of σ and λ.

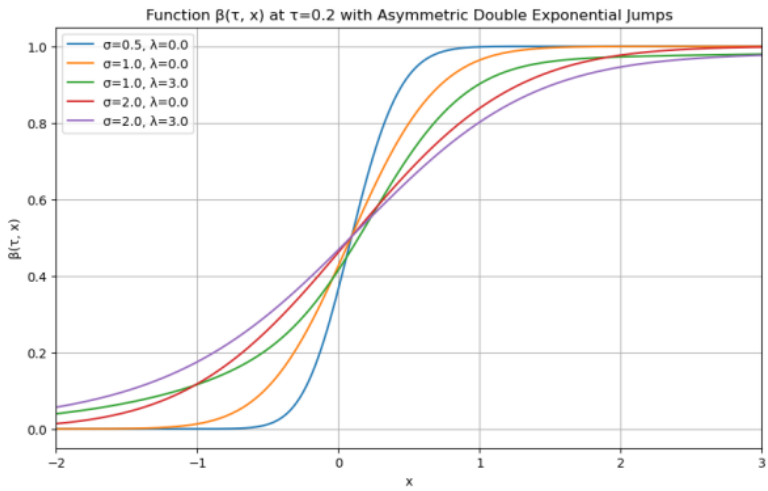

Figure 5: Plot of the function $\alpha(0.8, .)$ for varying values of σ and λ, considering a Double Exponential Distribution.

The notable differences are observed in the green and purple lines. The explanation for this phenomenon is straightforward. When the jump intensity (λ) is zero, the process exhibits no jumps, meaning that the prices of emission allowances ($A_t = \alpha(t, X_t)$) evolve continuously without abrupt discontinuities caused by information shocks or sudden events, such as revisions in allocations or shifts in demand. So, it does not matter if we are using a Normal distribution or a Double Exponential, since we do not have the part of the jumps. This scenario may be realistic in highly stable emission markets. However, it may underestimate the dynamics of markets like the EU ETS, where jumps are common.

The visual differences are particularly evident in the green and purple lines. Again, the symmetric normal distribution produces smooth and balanced $\alpha(t, x)$ curves, reflecting an even dispersion of jumps around zero. In contrast, the asymmetric double exponential distribution generates curves with a steeper upward inclination as maturity approaches, driven by a significantly higher probability of upward jumps compared to downward ones.

4.4 CGMY Model

In this section, we present the result obtained by adopting the CGMY (Carr-Geman-Madan-Yor) distribution as the model for the jumps in the pricing dynamics of emission allowances. This distribution stands out for its ability to capture the small, constant changes typical of these markets, providing a significant advantage over the double exponential distribution, which tends to emphasize more pronounced asymmetric jumps. With four parameters (C, G, M, and Y), the CGMY model offers considerable flexibility, allowing each parameter to influence the evolution of allowance prices in distinct ways, adapting to various market scenarios. To ensure model consistency, we determined the parameters to satisfy the following conditions:

$$E(Y) = C(M^{Y-1} - G^{Y-1})\Gamma(1-Y) = 0,$$

$$V(Y) = C(M^{Y-2} + G^{Y-2})\Gamma(2-Y) = 1,$$

assuming $0 < Y = 0.5 < 1$. Based on the properties of the Lévy process, we verified that, for this value of Y, the model exhibits complete monotonicity, infinite activity, and finite variation. To meet the first condition of zero expected value, we set $G = M = 5$, resulting in a symmetric distribution. Under these conditions, the parameter C was adjusted to 1.5958. The CGMY distribution is associated to the CGMY Lévy Process, and so the jump intensity (λ) is not fixed as in the previous jump-diffusion processes, being estimated differently as:

$$\lambda = \sum_{j=J_1}^{J_2} \nu_j, \tag{52}$$

where ν_j it will be calculated, using the formula (41), admitting only jumps above a certain value ϵ that defines the threshold for considering only jumps of greater magnitude. Recall that the Lévy measure in this case is $\nu(dy) = \lambda v(dy)$. This approach allows a focus on extreme events, aligning the model with the dynamics observed in emission markets. To have a more precise graph we assume $\epsilon = 0.00000001$. Based on these parameters, we generated the following graph:

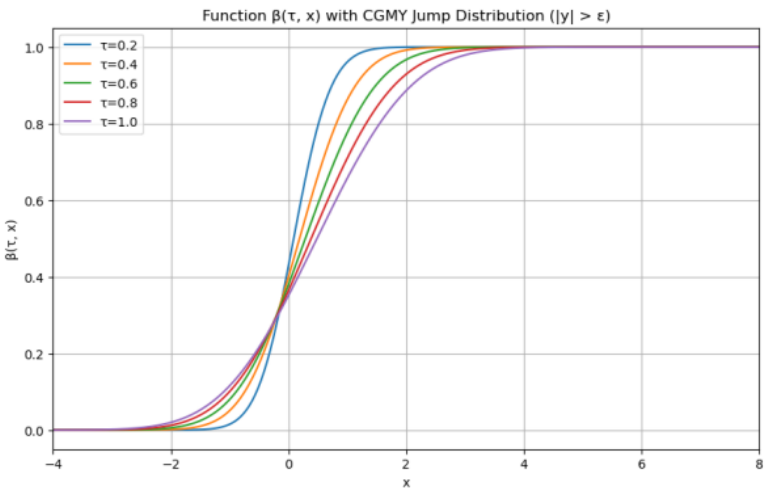

Figure 6: Plot of the function $\alpha(t, \cdot)$ for $t = 0, 0.2, 0.4, 0.6, 0.8$, calculated by discretization, with the parameters indicated, using the CGMY model.

The main differences compared to the graphs produced by the Standard Normal Distribution and the Double Exponential Distribution lie in the fact that the convergence to the extreme value π

was faster. This characteristic can be attributed to the heavy-tailed nature of the CGMY distribution, which incorporates a higher probability of significant jumps, affecting the price adjustment dynamics over time. This higher convergence reflects a greater resilience of the model to extreme shocks, providing a more nuanced representation of fluctuations in emission markets subject to regulatory uncertainties, and so, the uncertainty associated is much more higher then in the other two cases. Additionally, since the CGMY model has four parameters, it offers greater flexibility, allowing for more realistic pricing in line with prevailing market conditions.

5 Conclusion

The primary goal of this thesis was to develop a pricing model for carbon emission markets using a proposed jump-diffusion framework. This model aims to capture the evolution of emission allowance prices. To achieve this, we first introduce a discrete-time framework, outlining the essential processes associated with these markets. Subsequently, we transitioned to a continuous-time framework, which required defining an equilibrium market to describe price behavior as a function of the given processes and abatement strategies. This approach enabled the incorporation of jumps in a risk-neutral world, better capturing the abrupt shocks typical of these markets. To obtain the results, the associated partial integro-differential equation (PIDE) was discretized and implemented in Python. This work makes a significant contribution by offering an advanced tool for modeling emission allowance prices.

The results presented in this thesis, showed that when using a CGMY distribution to model the jumps, where the likelihood of major events causing sharp increases or decreases in allowance prices is higher, the convergence to the extreme values of π (the penalty level) and 0 was faster. This highlights the uncertainty tied to the heavy tails of this distribution. In contrast, the Double Exponential model showed a bit less stronger convergence toward the extreme value π, reflecting markets where the probability of events that lead to a shortage of allowances is much higher than the opposite. Meanwhile, despite its simplicity, the standard normal distribution struggled to capture extreme market conditions, making it more suitable for scenarios where we have moderate shocks. Thus, the comparative analysis reveals that the choice of jump distribution plays a critical role in shaping price dynamics, directly impacting the pricing of emission-related derivatives and risk management strategies.

Additionally, the study explored the influence, of varying diffusion terms (σ) and jump intensities (λ), in allowance prices across the Normal Distribution and the Double Exponential Distribution. It was found that higher values of these parameters accelerated convergence to extreme values, with the Double Exponential distribution showing the fastest convergence and the Standard Normal Distribution the slowest. This behavior highlights the increased uncertainty introduced by higher volatility and jump frequency.

Despite the advances presented, this thesis opens avenues for further research. Calibrating the CGMY model parameters to real-world EU ETS data could enhance the accuracy and realism of the price simulations. Additionally, exploring alternative abatement functions beyond the linear one adopted here could improve the representation of agents strategic behaviors in response to market conditions. For future research, investigating other Lévy processes, such as the Normal Inverse Gaussian or Variance Gamma (noting that the latter is a special case of the CGMY model), could provide further insights into price dynamics. Moreover, developing hedging strategies based on the derivative pricing insights derived from this model represents a promising direction for practical applications. By addressing these opportunities, future studies can build upon this work to enhance the robustness and applicability of emission allowance pricing models in volatile and evolving carbon markets.

6 Bibliography

References

[1] European Commission (2025), About the EU Emissions Trading System (EU ETS), *About the EU Emissions Trading System (EU ETS)*

[2] Chassagneux, J.-F., Chotai, H., Muuls, M. (2017) A Forward-Backward SDEs Approach to Pricing in Carbon Markets, SpringerBriefs in Mathematics of Planet Earth, Springer.

[3] Bento, A. (2022), Forward Backward Stochastic Differential Equations and Pricing in Emission Markets, MSc. Dissertation, ISEG, Universidade de Lisboa.

[4] D'Agua, J. (2023), Modelling Electricity and Emission Markets, MSc. Dissertation, ISEG, Universidade de Lisboa.

[5] Konstantin Borovkov, Geoffrey Decrouez and Juri Hinz (2011) Jump-Diffusion Modeling in Emission Markets, Stochastic Models, 27:1, 50-76, DOI: 10.1080/15326349.2011.542726

[6] Cont, R. and Tankov, P. (2004), *Financial Modelling with Jump Processes*, Chapman & Hall: New York.

[7] Wim Schoutens (2003), Lévy Processes in Finance: Pricing Financial Derivatives, John Wiley & Sons, Ltd.

[8] Kou, Steven G. (2002), A jump-diffusion model for option pricing, *Management science*, 48(8), 1086–1101, INFORMS.

[9] Peter Carr, Hélyette Geman, Dilip B. Madan, Marc Yor (2002), The Fine Structure of Asset Returns: An Empirical Investigation, Journal of Business.

[10] Hinz, J. and Novikov, A. (2010), On fair pricing of emission-related derivatives, *Bernoulli*, 16(4), 1240–1261.

[11] Hui-Hsiung Kuo (2006), *Introduction to Stochastic Integration*, Springer: New York.

[12] Gikhman, I.I. and Skorokhod, A.V. (1972), *Stochastic Differential Equations*, Springer-Verlag: New York.

[13] Applebaum, D. (2009), *Lévy Processes and Stochastic Calculus*, Cambridge University Press.

[14] La Chioma, C. and Briani, M. and Natalini, R. (2004), Convergence of numerical schemes for viscosity solutions to integro-differential degenerate parabolic problems arising in finance theory, *Numerische Mathematik*, 98(4), 607–646.

[15] Cont, Rama and Voltchkova, Ekaterina (2005), A Finite Difference Scheme For Option Pricing In Jump Diffusion And Exponential Lévy Models, *SIAM Journal on Numerical Analysis*, 43(4), 1596–1626, SIAM.

[16] Lancaster, P. (1969), *Theory of Matrices*, Academic Press: New York.

[17] Karatzas, I. and Shreve, S. (1991), *Brownian Motion and Stochastic Calculus*, 2nd Edition, Springer, Berlin.

[18] Cont, R., Tankov, P., and Voltchkova, E. (2007), *Hedging with Options in Models with Jumps*, In: Benth, F.E., Di Nunno, G., Lindstrøm, T., Øksendal, B., Zhang, T. (eds) *Stochastic Analysis and Applications*, Abel Symposia, vol 2, Springer, Berlin, Heidelberg.

Appendix A

To have a better understanding of how to use the Itô table and the Itô formula, it will be applied to the case where we do not have jumps.

From the discrete time framework provided by [10] it is reasonable to assume that the allowance price can be expressed in the functional form:

$$A_t = \alpha(t, X_t), \quad t \in [0, T],$$

where $\alpha : [0, T] \times \mathbb{R} \to \mathbb{R}$ is a suitable deterministic function. This allows the certificate price to be described as a deterministic function of time and state, facilitating the analysis. Now assuming that we are working in the case where we do not have jumps, we will have that, the state process $\{X_t\}_{t\in[0,T]}$ is given by

$$X_t := \varepsilon_t - \int_0^t r_s(A_s)\, ds, \quad t \in [0, T], \tag{53}$$

where ε_t is a martingale. In this case, by the martingale representation theorem, one must have

$$d\xi_t = \sigma_t\, dW_t, \tag{54}$$

for some admissible adapted process $\{\sigma_t\}_{t\in[0,T]}$, where$\{W_t\}_{t\in[0,T]}$ is a standard Brownian motion process (under $\mathbb{Q} \sim \mathbb{P}$) and $\{\mathcal{F}_t\}_{t\in[0,T]}$ is the natural filtration of the process. To make sure that $\{\varepsilon_t\}_{t\in[0,T]}$ has independent increments, we assume that $\{\sigma_t = \phi(t)\}_{t\in[0,T]}$ is deterministic and the abatement functions $r_t = r_t\}_{t\in[0,T]}$ are continuous nondecreasing time-independent. Now, to guarantee that A_t a martingale, we will apply the Itô's formula (Theorem 1) to achieve the conditions that the function α should satisfy. So,

$$dA_t = d\alpha(t, X_t) = \partial_{(1,0)}\alpha(t, X_t)\, dt + \partial_{(0,1)}\alpha(t, X_t)\, dX_t + \frac{1}{2}\partial_{(0,2)}\alpha(t, X_t)\, (dX_t)^2$$

By the Itô Table, since

$$d\varepsilon_t = \sigma_t dW_t,$$
$$dX_t = \sigma_t dW_t - r(\alpha(t, X_t))dt \implies (dX_t)^2 = \sigma_t^2 dt$$

and so,

$$dA_t = \partial_{(1,0)}\alpha(t, X_t)\, dt - \partial_{(0,1)}\alpha(t, X_t) r(\alpha(t, X_t))\, dt + \frac{1}{2}\partial_{(0,2)}\alpha(t, X_t)\sigma^2(t)\, dt + \partial_{(0,1)}\alpha(t, X_t)\sigma(t)\, dW_t =$$

$$(\partial_{(1,0)}\alpha(t, X_t) - \partial_{(0,1)}\alpha(t, X_t) r(\alpha(t, X_t)) + \frac{1}{2}\partial_{(0,2)}\alpha(t, X_t)\sigma^2(t))\, dt + \partial_{(0,1)}\alpha(t, X_t)\sigma(t)\, dW_t$$

To satisfy the martingale condition is essential to wipe out the drift term, which give us the following partial differential equation to $\alpha(t, x)$:

$$\partial_{(1,0)}\alpha(t, x) - \partial_{(0,1)}\alpha(t, x) r(\alpha(t, x)) + \frac{1}{2}\partial_{(0,2)}\alpha(t, x)\sigma^2(t) = 0. \tag{55}$$